CrossMark

Characterization, thermal properties and phase transitions of amazonian vegetable oils

Juliana J. R. Pardauil[1] · Fábio Alberto de Molfetta[3] · Miguel Braga[2] ·
Luiz K. C. de Souza[1] · Geraldo N. R. Filho[2] · José R. Zamian[2] · C. E. F. da Costa[2]

Abstract Thermal profiles of buriti pulp oil (*Mauritia flexuosa* Mart.), tucumã pulp and kernel oils (*Astrocarium vulgare* Mart.), rubber seed oil (*Hevea brasiliensis*), passion fruit oil (*Passiflora edulis*) and ucuúba butter (*Virola surinamensis*) were analyzed by thermogravimetry (TG/DTG) and differential scanning calorimetry (DSC). Gas chromatography and calculated iodine values were performed to determine the fatty acid profile and to measure the degree of unsaturation in these oils, respectively. The TG curves showed three steps of mass loss, which can be attributed to the degradation of polyunsaturated, monounsaturated and saturated fatty acids. The DSC crystallization and melting curves are reported and depended on the fatty acid composition. Usually, oil samples with a high degree of saturation showed crystallization and melting profiles at higher temperatures than the oils with a high degree of unsaturation. The data obtained by physicochemical analysis of oil samples were analyzed by principal component analysis and hierarchical cluster analysis to increase understanding of the data set, examining the presence or absence of natural groupings between samples.

Keywords DSC · Melting · Crystallization · PCA · HCA

Introduction

The Amazon region, with its richness of vegetable species, produces vegetable oils with unique aromas and flavors. The properties of these vegetable oils have been intensely researched, mainly by international companies, due to their various applications in food, pharmaceutical, cosmetic and other industries. Because the use of Amazonian vegetable oils has increased in recent years, it is important to acquire a better knowledge of their properties to optimize the use of these materials [1, 2].

Among the palm trees across the tropical region, the buriti (*Mauritia flexuosa* Mart.) can be highlighted. Buriti oil is an important source of proteins, energy and vitamins. The concentration of β-carotene corresponds to 90 % of the carotenoids present in the extracted pulp oil, which makes this oil effective in xerophthalmia treatment [3]. Additionally, this oil is commonly used to treat burns as a potent vermifuge and can be used as an adjuvant in sun protection [4].

The tucumã palm tree (*Astrocarium vulgare* Mart.) is found in Pará and Amapá states. Tucumã ripe fruits are orange, consisting of pulp and kernel which corresponding to approximately 53.2 and 24.5 %, respectively, of the fruit [5]. A micronutrient analysis showed that tucumã presents one of the highest concentrations of β-carotene, with 52 mg per 100 g of pulp; this concentration is approximately eight times higher than that found in carrots [6, 7].

✉ Juliana J. R. Pardauil
jpardauil@ufam.edu.br

1 Department of Chemistry, ICE, Federal University of Amazonas (UFAM), Av. Rodrigo Otávio, Campus Universitário Senador Arthur Vigílio Filho, Setor Norte, Coroado., Manaus, AM 69077-000, Brazil

2 Laboratory of Catalysis and Oil Chemistry, Department of Chemistry, Federal University of Para (UFPA), Rua Augusto Corrêa, 01 – Guamá, Belém, Pará 66075-110, Brazil

3 Laboratory of Molecular Modeling, Department of Chemistry, Federal University of Para (UFPA), Rua Augusto Corrêa, 01 – Guamá, Belém, Pará 66075-110, Brazil

The rubber tree (*Hevea brasiliensis*) originated from the basin of the Amazon River, but it is widely cultivated in Southeast Asia. Rubber seeds contain 17–20 % saturated fatty acids and 77–82 % unsaturated fatty acids, which gives it the characteristics of a semi-secant oil. Semi-secant oils provide quick sealing to treated surfaces [8].

Passion fruit (*Passiflora edulis*) is a tropical climate plant with a widespread geographical distribution, predominantly in regions with hot and humid climates, and is commonly cultivated in Brazil. Passion fruit oil has a yellow color, a pleasant flavor and a smooth odor, which is comparable to cotton oil in terms of nutritional level and digestibility, and the tea prepared by the infusion of the leaves has been recognized for its anti-inflammatory potential. Additionally, the oil is susceptible to oxidative rancidness due to the presence of a large amount of linoleic acid [9].

Ucuúba (*Virola surinamensis*) is a myristicaceous tree growing in the Amazonian flood plains and produces seeds during the rainy season. The fat extracted from the seeds (ucuúba butter) is rich in trimyristin. Phytochemical investigations on these species revealed the presence of steroids, flavonoids, polyketides, tetrahydrofuran lignans and one aryltetralinneolignan. Scientific studies are being conducted on the use of butter in the treatment of malaria and the trypanocidal activity against the trypomastigote forms of *Trypanosoma cruzi* [10].

Recently, thermal analytic methods, such as thermogravimetry/derivative thermogravimetry (TG/DTG) and differential scanning calorimetry (DSC), have been used to characterize oils and fats [11]. The DSC data of oils and fats have not given relevant information on the melting and crystallization temperatures as well as the heats of fusion and crystallization [12]. The phase transitions of lipids have been evaluated by DSC, mainly due to the observation of polymorphic transformations. Polymorphism in complex lipids is more complicated; the presence of a number of different triacylglycerols (TAGs) causes the coexistence of different fat crystals, including mixed crystals, which could undergo polymorphic transformations as a consequence of temperature changes [13]. Therefore, a consequence of the phenomenon of polymorphism is that the DSC melting curves of TAGs are not easily interpretable. Additionally, DSC crystallization curves are reproducible and simpler than melting curves because they are influenced only by the chemical composition of the oil or fat and not by the initial crystalline state [14].

The goal of this study was to evaluate the thermoanalytical profile (TG/DTG) and the phase transitions, melting and crystallization, of vegetable oils found in the Amazon region. These characteristics were investigated by DSC, and the thermal profiles were correlated with their compositions and it can be applied for use in the quality control of the vegetable raw material and for determining its feasibility for later use in cosmetic products, medicines and other industrial applications.

Materials and methods

Vegetable oils

Oil was extracted from the tucumã pulp (TP), tucumã kernel (TK) and rubber seeds (RS) using a Soxhlet apparatus and hexane as solvent. The passion fruit (PF), buriti pulp (BP) oils and ucuúba butter (UB) were obtained from a local oil provider, Amazon Oil Industry (Ananindeua, Pará, Brazil). These samples were unrefined and had no added preservatives. All of the chemicals and reagents used were of the highest purity.

Fatty acid determination (GC)

The fatty acid compositions of the oils were determined by gas chromatography (GC) using the AOCS Ce 1-62 method [15]. The fatty acid methyl esters were prepared by the AOCS Ce 2-66 method [16]. Chromatographic analysis was performed with a Varian CP 3800 gas chromatograph equipped with a hydrogen flame ionization detector and a capillary column (30 m × 0.32 mm CP WAX 52 CB; 1 µm DF) (California, USA). The column temperature was programmed to ramp from 80 to 250 °C at 10 °C min^{-1}, the injector temperature was set to 200 °C, and the detector temperature was set to 250 °C. Helium was used as the carrier gas.

Physicochemical characterization of oils

The physicochemical assays were performed in accordance with the standards established by the American Oil Chemists' Society (AOCS): acid value Cd 3d-63 [17]; peroxide value Cd 8-53 [18]; saponification value Tl 1a-64 [19]; and calculated iodine value—CIV–Cd 1c-85 [20]. The kinematic viscosity was determined using a thermostatic bath at 40 °C 52 SCHOTT coupled to a controller SCHOTT AVS 350 with a Cannon–Fenske routine viscometer that complies with standards ISO/DIS 3105, ASTM D 2515, BS 188 from SCHOTT Instruments (Mainz, Germany).

Thermal analysis

The thermogravimetric curves (TG/DTG) were obtained in a Shimadzu DTG 60H (Kyoto, Japan) simultaneous thermal analyzer (TG/DTG/DTA) by the dynamic method using an alumina crucible containing between 5 and 8 mg of oil sample and an empty alumina crucible as a reference.

The curves were recorded at a 10 °C min^{-1} heating rate, ranging from room temperature to 800 °C under synthetic air and nitrogen flow (50 mL min^{-1}).

DSC analyses were determined by a Shimadzu DSC-60 differential scanning calorimeter (Kyoto, Japan). The equipment was calibrated with pure indium (melting point 156.6 °C, $\Delta H_f = 28.45$ J g^{-1}) and n-dodecane (melting point -9.65 °C, $\Delta H_f = 216.73$ J g^{-1}), and the baseline was obtained with an empty hermetically sealed aluminum pan. An empty hermetically sealed aluminum pan was used as a reference. Samples of oils (5 $\pm$ 0.5 mg) were weighed into aluminum pans, and the covers were hermetically sealed into place.

For the TP, TK, BP and UB oil samples, the cooling and heating programs were: first heating the oil to 80 °C using a 10 °C min^{-1} heating rate and remaining 80 °C for 10 min to erase the crystal sample history, immediately followed by cooling to -80 °C using a 10 °C min^{-1} cooling rate and maintaining this temperature for 10 min and then heating at 10 °C min^{-1} to 80 °C. For the RS and PF oil samples, the cooling and heating program were: first heating the oil at 30 °C using a 10 °C min^{-1} heating rate and holding at 30 °C for 10 min, cooling to -100 °C using a 10 °C min^{-1} cooling rate and maintaining this temperature for 10 min and then heating at 10 °C min^{-1} to 30 °C. Nitrogen was the purge gas and flowed at 50 mL min^{-1}. Liquid nitrogen was used as the cooling agent. The curves were analyzed with a TA-60WS thermal analysis system (Shimadzu, Kyoto, Japan) to obtain the onset temperature (T_o), the offset temperature (T_f) (points where the extrapolated leading edge of the endotherm/exotherm intersects with the baseline), and the various peak temperatures (T_p) of the maximum/minimum different heat flows.

Statistical analysis

Principal component analysis (PCA) is based on the correlation among variables, and it is used to identify groups of analyzed variables, based on the factor loadings, i.e., correlations between the variables and the principal components (PCs) and groups of individuals based on the principal component scores. The score vectors describe the relationship between the samples and allow checking whether they are similar or dissimilar, typical or outlier, while the loading vectors describe the importance of each variable. The PCs are built as linear combination of the original independent variables and have the important property of being completely uncorrelated [21].

Hierarchical cluster analysis (HCA) examines the distances between the samples in a data set and represents this information as a two-dimensional plot called dendrogram. In HCA, the distances between samples or variables are calculated and compared through the similarity index which ranges from zero to one; a smaller distance means a larger index and therefore a larger similarity [21]. Statistical analysis (PCA and HCA) was performed using the software Minitab 15.

Results and discussion

The values obtained by gas chromatography for the chemical composition of the fatty acids in the vegetable oils are presented in Table 1. The analyzed oils had a high content of unsaturated fatty acids (62 % oleic acid for TP, 33 % linoleic acid for RS, 68 % linoleic acid for PF and 68.8 % oleic acid for BP), except for TK, which had a high content of saturated fatty acids that gave it the appearance of solid fat (48 % lauric acid and 25 % myristic acid). UB had approximately 71 % myristic acid. These oils can be classified as lauric fats. Lauric fats are commonly used in the food industry and oleochemical industry; palm kernel oil (PKO) is the most typical example of this category and is characterized by high contents of lauric and myristic acids. PKO and its fractions can be hydrogenated to different degrees to produce a wide range of PKO-based products, which are widely used in the food industry [22].

The high concentration of oleic acid found in TP and BP oils makes it useful for the food industry as a frying or salad oil. Additionally, oleic acid is an essential fatty acid (Omega 9) that participates in human metabolism, playing a key role in the synthesis of hormones; therefore, its inclusion in the diet is essential. RS oil displayed a fatty acid composition similar to linseed oil, whereas PF oil was found to be a good source of linoleic and linolenic acids. Linoleic and linolenic acids are essential in human

Table 1 Fatty acid compositions of oils

Fatty acid composition/%	Oils					
	UB	BP	TP	TK	RS	PF
12:0/Lauric acid	16		0.1	48		
14:0/Myristic acid	71		0.2	25		0.1
16:0/Palmitic acid	4.3	19.4	25	6	8.5	11
16:1/Palmitoleic acid	0.1		0.2			0.05
18:0/Stearic acid	0.7		3	2	5	3
18:1/Oleic acid	4	68.8	63	13.5	27	17
18:2/Linoleic acid	0.9	11.1	2	3.7	33	68
18:3/Linolenic acid		0.6	4		23	3.5
20:0/Araquidic acid	0.3		0.2	0.1	0.3	
22:0/Behenic acid					0.1	
SFA	92.4	19.4	28.5	81.1	13.5	14.1
MUFA	4.1	68.8	63.2	13.5	27	17.05
PUFA	0.9	11.7	6	3.7	56	71.5

nutrition because they represent a group of essential fatty acids, omega six and three, respectively. A deficient intake of these essential fatty acids causes dry, rough skin, a tendency for eczema and rash, weak hair, eventual alopecia and weak nails [23].

In Table 2, the physicochemical properties of the samples are shown. The acidic value and peroxide value are described as reference parameters to determine the quality of the conservation of oils. The Ministry of Health of Brazil (Ministério da Saúde-MS), through the National Health Surveillance Agency (Agência Nacional de Vigilância Sanitária-ANVISA), legalized the production of edible oils from an adopted technical regulation (resolution no. 270 of September 22, 2005) [24]. According to this resolution, the maximum acidic value and peroxide value for cold-pressed unrefined oils and fats is 4 mgKOH g^{-1} and 15 mEq kg^{-1}, respectively. The acidic and peroxide values for the analyzed samples are in agreement with the specifications of the Brazilian legislation, except for the acidic value found for UB. This high value can be attributed to the presence of resin in the uccúba butter, which contains large amounts of lignans and neolignans [25].

The saponification value and calculated iodine value are related only to the specific characteristics of each vegetable oil, such as the length of the chains and the number of unsaturation. If the oil or fat has fatty acids with a low molecular weight, the saponification value will be higher and more of the oil or fat can be used for food. The oils TP, RS, PF and BP showed high amounts of MUFA and PUFA and had high CIVs ($\geq$63.86). The lowest CIVs ($\leq$18.07) were for the fats TK and UB due to the high amounts of SFA. These fats also had the highest saponification values (236.4 and 235.5, respectively), whereas for the more unsaturated oils, the saponification value was $\geq$171.5.

The viscosity increases when the chain length of the fatty acid in the triglycerides is larger and decreases when unsaturation in the fatty acid chain is high. It is a function of the dimensions of the molecule and its orientation, i.e., it increases with hydrogenation. In the case of the studied oils, UB showed the highest kinematic viscosity (92.8 mm^2 s^{-1}) due to the high amounts of myristic acid. The palmitic acid content for BP, PF and RS is 19.4, 11 and

8.5 %, and the values for the kinematic viscosity were 38, 34 and 21.4 mm^2 s^{-1}, respectively.

Table 2 shows that data related to the physicochemical parameters were used for the principal component analysis (PCA) and hierarchical cluster analysis (HCA). Initially, was used the complete data set, i.e., the set containing all variables. Before applying the PCA method, all variables were autoscaled (focused on medium and scaled by the unit variance), so they can be compared with each other on the same scale.

The three variables responsible for the separation of oils were peroxide value, saponification value and calculated iodine value. The score graphs which are the new coordinates of each type of oil in the new coordinate system (PC) are shown in Fig. 1a. PCA results showed that first two PCs described 97.6 % of total information (variance) of the data set. PC1 is responsible for 66.6 % of the information, and PC2 has 31 % of information.

From the graph of the PCA scores can be observed the formation of three distinct classes of oils in relation to their physicochemical characteristics. Figure 5b shows the loading graphic for each one of the used variables in PCA analysis. When analyzing the score and loading graphics, it can be observed that the UB and TK samples were in the same quadrant, and the variable responsible for this separation was the saponification index.

Through score graphic, the samples UB and TK showed PC1 < 0 values, because these samples have high concentrations of saturated fatty acids. Also, RS, PF and BP samples showed positive values of PC1 and PC2 as shown in Fig. 1a, b and the responsible variable for the separation was CIV. High CIV values for these samples are related to their large content of unsaturated fatty acids. However, the TP sample had positive values in PC1, but negative in PC2; even noting that TP has a composition very similar in fatty acids in relation to the BP sample (Table 1). The physicochemical characteristic that describes this sample TP by the loading graph was the high peroxide value, as it is associated with the storage conditions of the fruits and the oil extraction process.

HCA dendrogram (Fig. 2) correlates with the results obtained by PCA plot, PC1 versus PC2. Figure 2 shows the

Table 2 Physicochemical analyses of oils

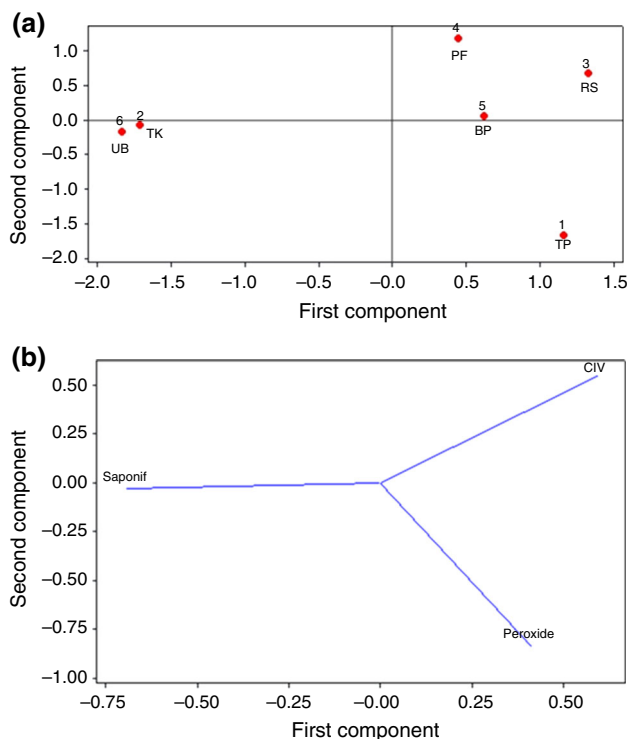| Physicochemical analyses	Oils					
	TP	TK	RS	PF	BP	UB
Acidic value/mgKOH g^{-1}	3.80	0.45	2.40	3.30	2.67	33.69
Peroxide value/mEq kg^{-1}	10.52	1.9	3.92	1.50	4.03	1.80
Saponification value/mgKOH g^{-1}	180.40	236.40	171.55	193.86	175.50	235.50
Kinematic viscosity/mm^2 s^{-1}	19.40	15.40	21.40	33.60	38.04	92.80
CIV	67.77	18.07	140.26	133.85	79.96	5.05

Fig. 1 Plot of the first two score vectors (**a**) and (**b**) loading vectors (PC1 and PC2) of the variables responsible for the separation of the oils
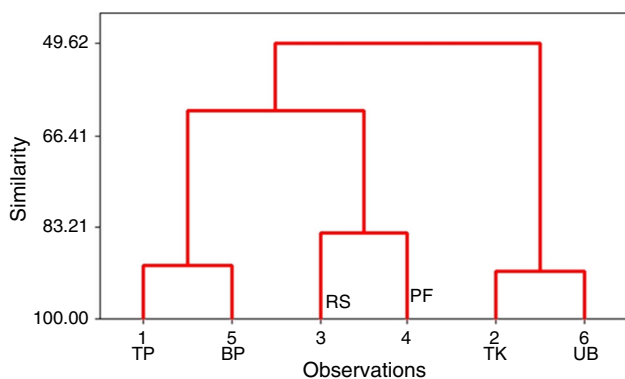

Fig. 2 Dendrogram obtained with HCA for the sample oils

Fig. 3 TG (*a*) and DTG (*b*) curves for the oils in a synthetic air atmosphere
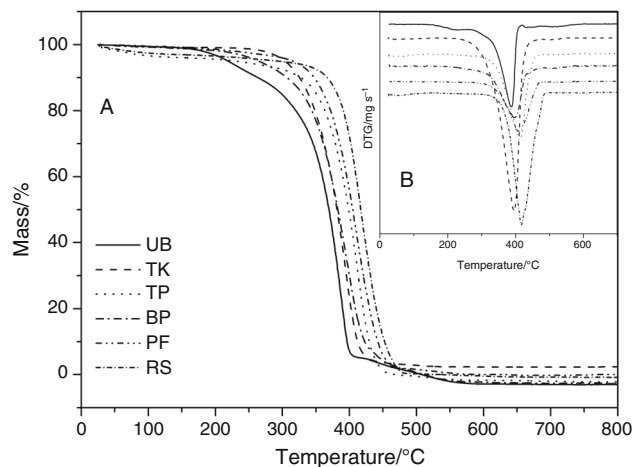
Fig. 4 TG (*a*) and DTG (*b*) curves for the oils in an N_2 atmosphere

highest similarity among TP and BP, PF and RS and between TK and UB samples probably due to the fatty acids similarities as TP and BP have 63.2 and 68.8 % of MUFA, PF and RS have 56 and 71.5 % of PUFA, and TK and UB have 81 and 92 % of SFA, respectively.

The thermal behaviors for the oils are displayed in Figs. 3a, b and 4a, b. According to the TG/DTG curves, a ramp of thermal stability of the oil was observed to approximately 200–290 °C. Until this temperature, the mass loss corresponds to the removal of water, moisture and volatilization of substances, such as fatty acids with 12–16 carbons in the chain [26]. The TG/DTG curves
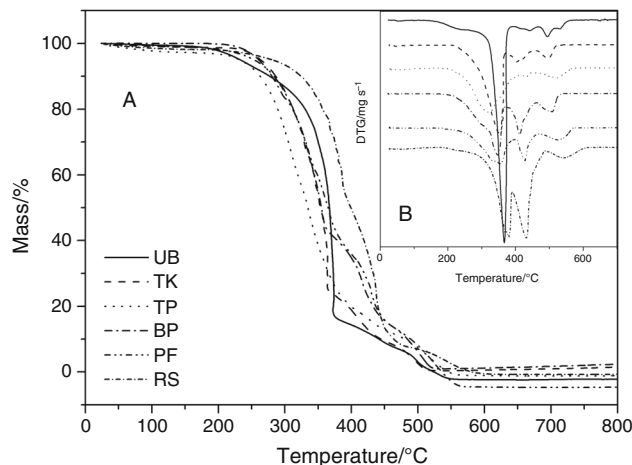
showed that in an air atmosphere, the thermogravimetric profile presented three decomposition steps, whereas in an N_2 atmosphere, there were only one or two steps, suggesting that in an oxidizing atmosphere, the decomposition process occurs by combustion, and in an inert atmosphere, thermodecomposition occurs by pyrolysis.

In the TG curves, the initial temperature (T_i) of the first stage of mass loss for the UB, TK, TP, BP, PF and RS, respectively, was:

- Air atmosphere: 204; 260; 257; 268; and 296 °C.
- N_2 atmosphere: 225; 295; 322; 350; and 370 °C.

For UB, TK TP and BP, the T_i values were smaller in both atmospheres than for PF and RS. This may be related to the volatilization of lauric, myristic and palmitic acids present in significant amounts in these oils. In this case, T_i may not necessarily be associated with the thermal decomposition. [27] ascribed these steps to the following

processes: (1) decomposition of polyunsaturated fatty acids, such as linoleic acid, with the formation of compounds, such as dimers, trimers and polymers; (2) decomposition of monounsaturated fatty acids, such as oleic acid; and (3) decomposition of saturated fatty acids, such as palmitic acid. Other authors considered that all three types of fatty acids decompose in the first step. However, others authors attributed the last stage of decomposition to the oxidation of carbon residues [28, 29]. Garcia et al. [30] reported the first and second mass loss steps as the oxidation of unsaturated and saturated fatty acids, respectively, whereas the third step was related to the decomposition of polymers formed during the oxidation process. However, according to Vecchio et al. [31], the results of these studies are often contradictory because vegetable oils have a complex chemical composition, including lipid oxidation products, free fatty acids, phenolic compounds, glycerides and non-glycerides, which are present in the oil at different percentages; therefore, a clear assignment of each event as a decomposition of a certain chemical species is difficult if only analyzing the profile of the TG/DTG curves because the mass losses of various chemical components due to the decomposition of lipids most likely occur at the same time during each step.

Crystallization curves often exhibit multiple exothermic regions corresponding to different triacylglycerol compositions. Melting causes a volume expansion and an endothermic effect. Additionally, a complex feature of triglycerides makes the melting process difficult to interpret in relation to the crystallization process due to the presence of overlapping peaks [32]. This is a consequence of the polymorphism phenomena of natural oils and fats, and this cannot be established unequivocally by DSC measurements. Only X-ray diffraction analysis can determine the exact polymorphic form [32, 33]. DSC cooling curves for the studied oils are shown in Fig. 5a, b. The main transition parameters as well as the enthalpy for the crystallization curves are shown in Table 3. In UB, the crystallization curve showed two exothermic overlapping peaks: the larger one centered at 16.5 °C and the smaller one centered at 11.4 °C. These peaks in the high-temperature regions occur due to the high concentration of SFA, mainly myristic and lauric acids, which are the main constituents in this butter. The crystallization curve for TK exhibits two distinct exothermic peaks: the taller peak had a T_p at approximately 6 °C, and the short one had a T_p at −9 °C. These peaks occur due to the presence of TAGs with three chains of SFA, such as lauric, myristic and palmitic acids. Following these peaks can be observed a small peak around −29 °C, most likely due to the crystallization of TAGs containing chains of MUFA and PUFA. The TP crystallization curve exhibited three exothermic transitions. The first was a sharp and narrow
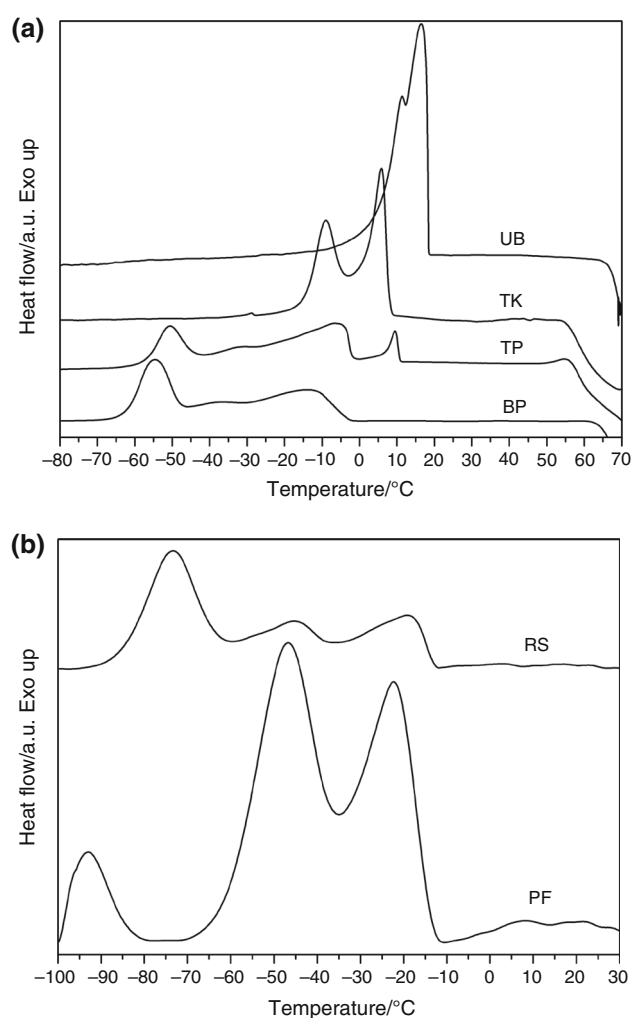

Fig. 5 DSC cooling curves for the studied oils **a** UB, TK, TP, BP and **b** RS, PF

peak around at 11 °C, which can be related to the amount of SFA (28.5 %) in this oil. The second was a broader peak centered at −6.6 °C and followed by a smooth shoulder at −33 °C. The last peak at −50.5 may correspond to groups of TAGs with saturated–saturated–unsaturated, saturated–unsaturated–unsaturated and unsaturated–unsaturated–unsaturated chains of fatty acids [14]. In BP, the crystallization pattern was similar to TP oil, except for the absence of the exothermic peak in the high-temperature region. The first broad peak had a T_p at −12.9, followed by a shoulder at −37 °C, and the last peak was taller and had a T_p at −54 °C. These peaks may be associated with the presence of the same groups of TAGs contained in TP oil, mainly because of the high content of oleic acid. Likewise, the RS crystallization curve had three exothermic regions at −19.2, −45.4 and −73.4 °C, respectively, consistently lower than the other crystallization curves, most likely due to the high amount of linolenic acid. The PF curve showed three exothermic peaks at −16.3, −39 and −93 °C, but

Table 3 DSC parameters of the main peaks and enthalpy from the cooling curves of the oil samples

Oils	1° peak T/°C			2° peak T/°C			3° peak T/°C			ΔH_T/J g^{-1}
	T_o	T_p	T_f	T_o	T_p	T_f	T_o	T_p	T_f	
UB	18.5	16.5	7.6							−107.82
TK	8.1	5.9	1.8	−5.1	−9.0	−15.5				−108.22
TP	11.2	9.5	6.1	−1.7	−6.6	−19.4	−44.5	−50.5	−57.2	−61.95
BP	−5.1	−12.9	−28.8	−50.5	−54.0	−59.9				−66.61
RS	−13.1	−19.2	−32.8	−38.5	−45.4	−56.4	−64.0	−73.4	−85.1	−5.82
PF	−16.3	−20.3	−32.1	−39.0	−46.2	−58.6	−78.7	−93.1	−97.7	−19.25

ΔH_T: total cooling enthalpy

these peaks were sharper and taller than those present in the RS crystallization, possibly due to the greater amount of unsaturated fatty acid contained in PF. Also, Tengku-Rozaina and Birch [34] analyzing fractionated refined hoki oil observed that DSC curves of crystallization peaks for the fraction containing higher percentage of unsaturated fatty acids tend to be shifted to the lower-temperature regions.

Due to the complexity of the melting curves, the thermal events were read at the minimum of the endothermic peaks (Table 4). The DSC melting curves are shown in Fig. 6a, b. All of the curves showed multiple endothermic events related to the different TAG compositions of the oils. The UB melting curve had three main endothermic peaks. The first peak was at 21.5 °C, most likely indicating the fusion of TAGs with short chain fatty acids, such as lauric acid, followed by a taller exothermic peak that indicates a polymorphic event, i.e., a rearrangement of polymorphic crystals into more stable forms [32]. According to Tolstorebrov et al. [35], the typical DSC melting curves include the endothermic and exothermic peaks, which show the transition of one form of fat crystals into another. In this way, this event can be related to the melting of α-crystals followed by β-crystal formation (exothermic peak in the UB melting curve). The second endotherm located at the high-temperature region was formed by two overlapped peaks at 30.8 and 37.2 °C and may be associated with the melting of TAGs containing

myristic and palmitic chains. The TK and TP melting profiles were similar to those found by Tan and Che Man [32] for palm kernel oil and palm oil at the same heating rate. The TK heating curve presented one main endothermic transition at 28 °C with two slight shoulders at 14.5 and 39 °C. This major endothermic peak was the fusion of TAGs with saturated fatty acids with high melting points present in lauric fats [22]. The heating curve of TP showed two major endotherm regions. This can be matched to the endothermic transitions of MUFA, such as oleic acid (lower-temperature peak) and SFA, e.g., palmitic acid (higher temperature region). The endothermic region at higher temperature consisted of a plateau with a pair of shoulders, whereas the endotherm region at lower temperature contained three overlapped peaks. In contrast, BP oil exhibited a main endothermic domain at −4.7 °C preceded by two shoulders at −54 and −36.9 °C and an exothermic polymorphic transition at approximately −30 °C. RS and PF were the most unsaturated oils and presented four and seven endothermic domains at low temperatures, respectively. RS had a main endothermic peak with two shoulders that can be associated with the highly cooperative melting of TAGs containing chains of oleic, linoleic and linolenic fatty acids. The fourth endothermic peak, consistently lower than the others, at 7.5 °C can be related to the fusion of SFA, which makes up 13.5 % of this oil. For PF, the principal melting process happens below −20 °C, and the broadening of the

Table 4 DSC transition temperatures and enthalpy from the melting curves of the oil samples

Oils	Transition temperatures/°C							ΔH_T/J g^{-1}
	1	2	3	4	5	6	7	
UB	21.5	30.8	37.2					119.66
TK	14.5	28.0	39.0					117.35
TP	−36.4	−4.7	2.4	15.3	31.8			88.69
BP	−54.0	−36.9	−4.7					91.44
RS	−33.2	−22.1	−11.2	7.5				18.47
PF	−92.6	−79.4	−62.8	−40.2	−31.5	−18.8	−9.8	37.30

ΔH_T: total meting enthalpy

Fig. 6 DSC heating curves for the studied oils **a** UB, TK, TP, BP and **b** RS, PF

Conclusions

It was confirmed that the melting and crystallization characteristics of oils and fats were strongly dependent on the FA and TAG compositions. The DSC technique does not provide direct information about the chemical composition of oils and fats. However, it provides useful information about the nature of the thermodynamic changes associated with phase transitions that are related to the composition of oils and fats. The methods of multivariate analysis PCA and HCA allowed a comparison between physicochemical characteristics of the samples that are related to chemical fatty acid composition of the oils studied.

References

1. Pardauil JJR, Souza LKC, Molfetta FA, Zamian JR, Rocha Filho GN, Costa CEF. Determination of the oxidative stability by DSC of vegetable oils from the Amazonian area. Bioresour Technol. 2011;102:5873–7.
2. Santos OV, Corrêa NCF, Carvalho RN Jr, Costa CEF, França LFF, Lannes SCS. Comparative parameters of the nutritional contribution and functional claims of Brazil nut kernels, oil and defatted cake. Food Res Int. 2013;51:841–7.
3. Cunha MAE, Neves RF, Souza JNS, França LF, Araújo ME, Brunner G, Machado NT. Supercritical adsorption of buriti oil (*Mauritia flexuosa* Mart.) in—alumina: a methodology for the enriching of anti-oxidants. J Supercrit Fluids. 2012;66:181–91.
4. Forero-Doria O, Gallego J, Valdes O, Pinzon-Topa C, Santos LS, Guzma L. Relationship between oxidative stability and antioxidant activity of oil extracted from the peel of *Mauritia flexuosa* fruits. J Therm Anal Calorim. 2016;123:2173–8.
5. Lima JRO, Silva RB, Moura EM, Moura CVR. Biodiesel of tucum oil, synthesized by methanolic and ethanolic routes. Fuel. 2008;87:1718–23.
6. Lira CS, Berruti FM, Palmisano P, Berruti F, Briens C, Pécora AAB. Fast pyrolysis of Amazon tucumã (*Astrocaryum aculeatum*) seeds in a bubbling fluidized bed reactor. J Anal Appl Pyrol. 2013;99:23–31.
7. Souza Filho OC, Sagrillo MR, Garcia LFM, Machado AK, Cadona F, Ribeiro EE, Duarte MMMF, Morel AF, Cruz IBM. The in vitro genotoxic effect of Tucuma (*Astrocaryum aculeatum*), an Amazonian Fruit Rich in Carotenoids. J Med Food. 2013;16:1013–21.
8. Salimon J, Abdullah BM, Salih N. Rubber (*Hevea brasiliensis*) seed oil toxicity effect and Linamarin compound analysis. Lipids Health Dis. 2012;11:74.
9. Silva JK, Cazarin CBB, Colomeu TC, Batista AG, Meletti LMM, Paschoal JAR, Bogusz S Jr, Furlan MF, Reyes FG, Maróstica MR Jr, Zollner RL. Antioxidant activity of aqueous extract of passion fruit (*Passiflora edulis*) leaves: in vitro and in vivo study. Food Res Int. 2013;53:882–90.

endotherms is due to the overlap of several melting transitions of highly polyunsaturated moieties followed by the melting of monounsaturated fatty acids and a small fraction of saturated fatty acids. Additionally, in the temperature region below −60 °C, there is a polymorphic transition represented by two exothermic peaks at −85 and −70 °C. The crystallization and melting enthalpies are given in Tables 3 and 4, respectively. Oils with high degrees of saturation, such as UB, TK, TP and BP, had DSC melting enthalpies at higher values than the oil samples with high degrees of unsaturation (RS and PF oils). This occurs because the oils with high saturation degrees require more energy during the melting process. Additionally, the higher crystallization enthalpy for the samples with a large amount of SFA was caused by a more ordered crystal structure because TAG chains are more compactly associated.

10. Stecanella LA, Taveira SF, Marreto RN, Valadares MC, Vieira MS, Kato MJ, Lima EM. Development and characterization of PLGA nanocapsules of grandisin isolated from *Virola surinamensis*: in vitro release and cytotoxicity studies. Braz J Pharmacogn. 2013;23:153–9.

11. Samyn P, Schoukens G, Vonck L, Stanssens D, Van den Abbeele H. Quality of Brazilian vegetable oils evaluated by (modulated) differential scanning calorimetry. J Therm Anal Calorim. 2012;110:1353–65.

12. Sessa DJ. Derivation of a cocoa butter equivalent from Jojoba transesterified ester via a differential scanning calorimetry index. J Sci Food Agric. 1996;72:295–8.

13. Calligaris S, Arrighetti G, Barba L, Nicoli MC. Phase transition of sunflower oil as affected by the oxidation level. J Am Oil Chem Soc. 2008;85:591–8.

14. Tan CP, Che Man YB. Differential scanning calorimetric analysis of edible oils: comparison of thermal properties and chemical composition. J Am Oil Chem Soc. 2000;77:143–55.

15. American Oil Chemists' Society. Official methods and recommended practices of the American Oil Chemists' Society. 4th ed. Champaign, USA (A.O.C.S.Official Method Ce 1-62: Fatty acid composition by gas chromatography); 1995.

16. American Oil Chemists' Society. Official methods and recommended practices of the American Oil Chemists' Society. 4th ed. Champaign, USA (A.O.C.S.Official Method Ce 2-66: Preparation of methyl esters of long chain fatty acids); 1995.

17. American Oil Chemists' Society. Official methods and recommended practices of the American Oil Chemists' Society. 5th ed. Champaign, USA (A.O.C.S.Official Method Cd 3d-63: Acid value); 1999.

18. American Oil Chemists' Society. Official methods and recommended practices of the American Oil Chemists' Society. 4th ed. Champaign, USA (A.O.C.S.Official Method Cd 8-53: Peroxide value); 1997.

19. American Oil Chemists' Society. Official methods and recommended practices of the American Oil Chemists' Society. 4th ed. Champaign, USA (A.O.C.S.Official Method AOCS Tl 1a-64: Saponification Value); 1997.

20. American Oil Chemists' Society. Official methods and recommended practices of the American Oil Chemists' Society. 5th ed. Champaign, USA (A.O.C.S.Official Method AOCS Cd 1c-85: Calculated Iodine Value); 1997.

21. Molfetta FA, Bruni AT, Honório KM, Silva ABF. A structure–activity relationship study of quinone compounds with trypanocidal activity. Eur J Med Chem. 2005;40:329–38.

22. Anihouvi PP, Blecker C, Dombree A, Danthine S. Comparative study of thermal and structural behavior of four industrial lauric fats. Food Bioprocess Technol. 2013;6:3381–91.

23. Regitano-d'Arce MAB. Química básica dos lipídeos. In: Oetterer M, Regitano-d'Arce MAB, Spoto MHF, editors. Fundamentos de ciência e tecnologia de alimentos. Manole, Barueri-SP; 2006. p. 196–242.

24. BRASIL. Resolução RDC/ANVISA/MS n° 270, de 22 de setembro de 2005. Regulamento técnico para óleos vegetais, gorduras vegetais e creme vegetal. Diário Oficial da República Federativa do Brasil. Brasília, DF, 23 setembro 2005. Seção 1.

25. Lopes NP, Kato M, Yoshida M. Antifungal constituents from roots of *Virola surinamensis*. Phytochemistry. 1999;51:29–33.

26. Costa MNFS, Muniz MAP, Negrão CAB, Costa CEF, Lamarão MLN, Morais L, Silva Jr JOC, Costa RMR. Characterization of *Pentaclethra macroloba* oil: thermal stability, gas chromatography and Rancimat. J Therm Anal Calorim. 2014;115:2269–75.

27. Santos JCO, Santos IMG, Souza AG, Prasad S, Santos AV. Thermal stability and kinetic study on thermal decomposition of commercial edible oils by thermogravimetry. J Food Sci. 2002;67:1393–8.

28. Dweck J, Sampaio CMS. Analysis of the thermal composition of commercial vegetable oils in air by simultaneous TG/DTA. J Therm Anal Calorim. 2004;75:419–28.

29. Santos AGD, Caldeira VPS, Souza LD, Oliveira DS, Araujo AS, Luz GE Jr. Study of the thermal stability by thermogravimetry for oil, biodiesel and blend (B10) of different oilseeds. J Therm Anal Calorim. 2016;123:2021–8.

30. Garcia CC, Franco PIBM, Zuppa TO, Antoniosi Filho NR, Leles MIG. Thermal stability studies of some cerrado plant oils. J Therm Anal Calorim. 2007;87:645–8.

31. Vecchio E, Cerretani L, Bendini A, Chiavaro E. Thermal decomposition study of monovarietal extra virgin olive oil by simultaneous thermogravimmetry/differential scanning calorimetry: relation with chemical composition. J Agric Food Chem. 2009;57:4793–800.

32. Tan CP, Che Man YB. Differential scanning calorimetric analysis of palm oil. Palm oil based products and coconut oil: effects of scanning rate variation. Food Chem. 2002;76:89–102.

33. Kobelnik M, Fontanari GG, Soares RAM, Figueiredo AG, Ribeiro CA. Study of the thermal behavior of bicu'ba oil (*Virola bicuhyba*). J Therm Anal Calorim. 2014;115:2107–13.

34. Tengku-Rozaina TM, Birch EJ. Effects of fractionation on melting and crystallisation profiles of hoki oil measured by DSC. J Therm Anal Calorim. 2015;120:395–402.

35. Tolstorebrov I, Eikevik TM, Bantle M. A DSC determination of phase transitions and liquid fraction in fish oils and mixtures of triacylglicerides. Food Res Int. 2014;58:132–40.